Tetrahedron xxx (xxxx) xxx

Contents lists available at ScienceDirect

Tetrahedron

journal homepage: www.elsevier.com/locate/tet

# Pillar[5]arene-BODIPY host-guest interaction induced fluorescence enhancement and lysosomes targetable bioimaging in dilute solution

Jia-Yi Chen [a], Xing-Yu Li [a], Jie Wu [b], Yongquan Wu [b, **], Gui-Chao Kuang [a, c, *]

[a] State Key Laboratory of Power Metallurgy, Central South University, Changsha, Hunan, 410083, PR China
[b] Key Laboratory of Organo-pharmaceutical Chemistry, School of Chemistry and Chemical Engineering, Gannan Normal University, Ganzhou, Jiangxi, 341000, PR China
[c] State Key Laboratory of Molecular Engineering of Polymers, Fudan University, Shanghai, 200438, PR China

ARTICLE INFO

*Article history:*
Received 3 August 2020
Received in revised form
12 October 2020
Accepted 16 October 2020
Available online xxx

*Keywords:*
BODIPY
pillar[5]arenes
Host-guest
Aggregation induced emission
Supramolecular chemistry
Bioimaging

ABSTRACT

Supramolecular complex by pillar[5]arenes and BODIPY dyad through host-guest interaction was developed and showed aggregation induced emission (AIE) property. $^{1}$H NMR titration and 2D NOESY NMR measurements were performed to evidence the host-guest interaction and the complex was formed by 1:1 M ratio. The fluorescence intensities of the BODIPY dyad were enhanced by increasing solution viscosity or and host-guest supramolecular interaction with pillar[5]arenes. Preliminary living cell imaging results demonstrated the highly emissive complex showed lysosome targetable property.



## 1. Introduction

4,4-difluoro-4-bora-3a,4a-diaza-*s*-indacene (BODIPY) dyads have gained great attention in the last three decades due to their excellent photophysical properties [1] and various applications [2]. Through structural modification, these BODIPY dyads showed tunable photophysical properties and three well-reported strategies were developed to regulate these dyads' fluorescent emission intensities and wavelength [3]. For the BODIPY dyads containing donor or acceptor structural moieties, their fluorescence emissions were quenched by photoinduced electron transfer (PET) [4–6]. After binding or reacting with a chemical, the electron transfer pathway was blocked and thus fluorescent emission was restored. Therefore, these BODIPY dyads could be used as fluorescent probes [7]. Charge transfer (CT) is the second strategy to tune their photophysical properties [8]. These dyads' fluorescence properties were highly correlated with their environment such as solution temperature, solvents viscosity and polarity, etc. The third strategy to influence BODIPY dyads emissions by restricting the intramolecular rotation at the *meso* position has just been recognized about ten years [9–11]. To make these aggregation induced emission (AIE) dyads to be highly emissive was usually by adding poor solvents, increasing the solvents viscosity or decreasing temperature [12–14]. Although some progress has been made in this area, there are few reports referring to using host-guest interaction to get highly emissive BODIPY complex. Due to the BODIPY dyads large size, it is difficult to select a suitable host to capture BODIPY guest [15,16]. Therefore, to develop supramolecular host-guest system to make BODIPY highly emissive in solution remains interesting and challenging.

On the other hand, five kinds of macrocycles behaved as supramolecular hosts have been demonstrated [17,18]. In the past decade or so, the pillararene-based host-guest chemistry has been intensively and extensively studied [19]. These macrocycles have shown a wide range of applications in supramolecular hosts due to their easy tunable cavity size. The repeating unit could be changed from 5 to 15 [20]. In addition, appropriate outer structural modification led to these macrocycles to be water soluble, which would be very important for these host-guest complexes biological application [21]. For example, the host-guest complexes between P

* Corresponding author. State Key Laboratory of Power Metallurgy, Central South University, Changsha, Hunan, 410083, PR China.
** Corresponding author.
*E-mail addresses:* wyq@gnnu.edu.cn (Y. Wu), gckuang@csu.edu.cn (G.-C. Kuang).

https://doi.org/10.1016/j.tet.2020.131698
0040-4020/

Please cite this article as: J.-Y. Chen, X.-Y. Li, J. Wu *et al.*, Pillar[5]arene-BODIPY host-guest interaction induced fluorescence enhancement and lysosomes targetable bioimaging in dilute solution, Tetrahedron, https://doi.org/10.1016/j.tet.2020.131698

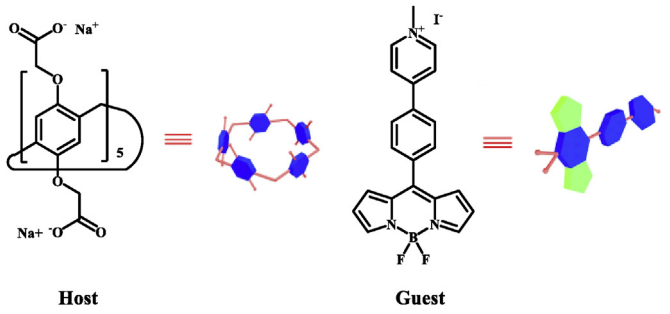


**Scheme 1.** Molecular structures and cartoon representation of BDP-1 and P[5].

[5] hydrophobic anticancer drug tamoxifen could be efficiently delivered to cancer cells and showed enhanced pesticide effect [22]. Inspired by the well-known AIE fluorogen tetraphenylethene derivatives exhibited strong fluorescent emission with P[5] [23,24], herein, we designed a BODIPY dyad with pyridinium unit at *meso* position. Considering the similar structural moiety baring at the different dye, we expected that this BODIPY dyad could form host-guest supramolecular complex with P[5].

Our group has been interested in water soluble BODIPY derivatives since 2014 [25–32]. We found the dendritic oligo(ethylene glycol) modified BODIPY showed enhanced fluorescent intensity during the thermoresponsive process [25]. Detailed photophysical studies demonstrated that, due to dehydration of oligo(ethylene glycol), the microviscosity around the BODIPY dyad increased, which restricted the intramolecular rotation and hampered photoelectron transfer pathway. In this work, a novel BODIPY derivative **BDP-1** was prepared and its host-guest complex with water soluble **P[5]** was investigated (Scheme 1). **BDP-1** showed enhanced fluorescence emission in viscous solutions. The supramolecular complex formed by **BDP-1** and **P[5]** through host-guest interaction was examined by Proton nuclear magnetic resonance ($^1$H NMR) titration and 2D nuclear Overhauser effect spectroscopy (NOESY) NMR. The fluorescent intensities of the complex exhibited gradually enhancement during the **P[5]** addition. Preliminary living cell imaging results demonstrated the highly emissive complex could stain lysosomes specifically.

## 2. Results and discussions

### 2.1. Synthesis and characterization

**BDP-1** was synthesized through three steps reaction (Scheme 2). Starting from 4-bormobenzaldehyde (**1**) and 4-pyridylboronic acid (**2**), compound **3** could be obtained after Suzuki coupling reaction with catalytic palladium triphenylphosphine. Thereafter, one pot classic acid-catalysis condensation, oxidation by *p*-chloranil and complexation with boron trifluoride etherate ($BF_3{\cdot}Et_2O$) reactions gave rise to BODIPY derivative **4**. Followed by reaction with iodomethane, our target guest molecule **BDP-1** was obtained. While the host molecule **P[5]** was synthesized according to reported procedure (Scheme 3) [33]. Detailed synthesis and characterization for both host and guest molecules have been demonstrated in Experimental section.

### 2.2. Photophysical properties

The photophysical properties of **BDP-1** in various polarity solvents and viscous solution were investigated. Charge deficient methyl pyridium unit behaves as acceptor while BODIPY fluorogen becomes as donor. Therefore, strong CT effect would lead to **BDP-1**

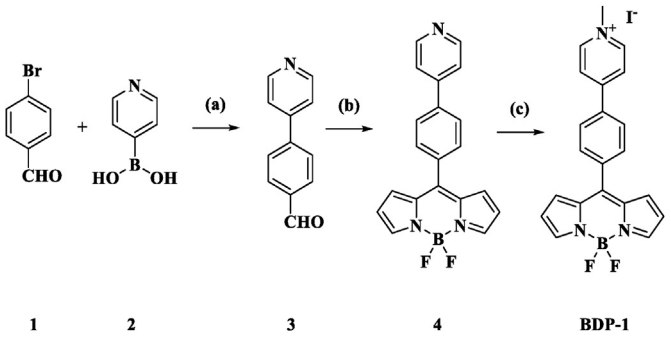


**Scheme 2.** Synthetic route for BDP-1.

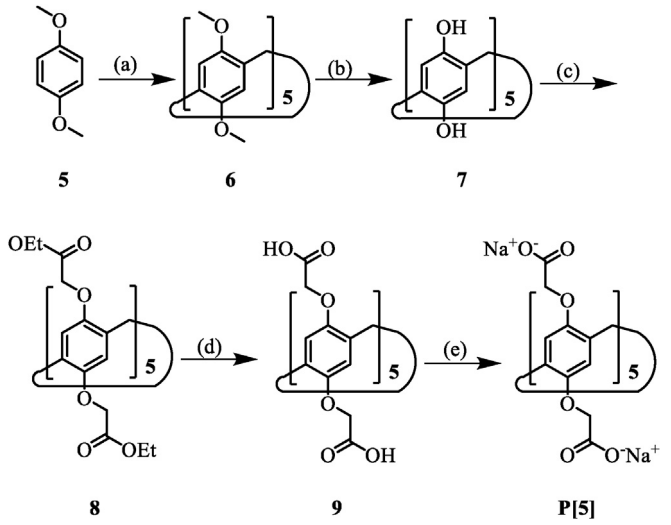


**Scheme 3.** Synthetic route for P[5].

be sensitive to solvents polarity. The fluorescence spectra of **BDP-1** were collected and showed apparent solvents dependent (Fig. S1). Weak fluorescent emission could be detected in polar solvents such as methanol, *N*,*N*-dimethylformide (DMF), acetonitrile (MeCN) and dimethylsulfoxide (DMSO), but strong fluorescent emission was observed in non-polar dioxane and carbon tetrachloride.

The fluorescence properties of **BDP-1** were correlated to the solvents viscosity as well. Due to rotation of the single bond between the phenyl linkage and BODIPY in free state, **BDP-1** showed weak emission in good solvents because the energy was lost through non-radioactive pathway. In viscous solution or aggregated state, the intramolecular rotation was restricted and the fluorescence intensity would be restored. Therefore, the photophysical properties in mixture solvents were investigated. When the **BDP-1** was dissolved in water/THF mixture solvents, the fluorescence emission intensities increased gradually with the fraction of water increase, indicating the formation of **BDP-1** aggregate. However, the intensity was still weak even when the fraction of water reached 99% (Fig. 1a). These results demonstrated that **BDP-1** showed good dispersity in polar aqueous solution because of the hydrophilic pyridinium units. Therefore, we further conducted another fluorescent measurement by dissolving **BDP-1** in glycerol/water with varying fraction of viscous glycerol. Naked eye observation revealed dramatic intensities changes (Fig. S2). Further quantitative measurements were performed by fluorescent spectra, which showed about $10^5$ times intensity enhancement (Fig. 1b). Two preliminary conclusions could be drawn from these results.

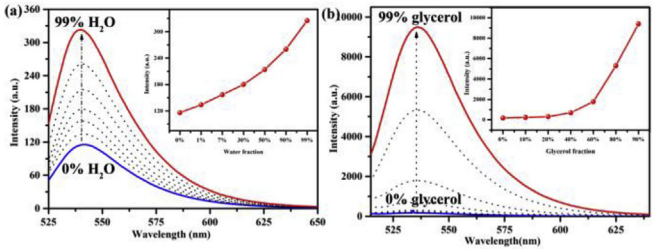


**Fig. 1.** Fluorescent spectra of BDP-1 in (a) water/THF; (b) glycerol/water mixture solvents. Condition: concentration is 1 $\mu$M, excitation wavelength is 504 nm, slits are 10 nm/10 nm.

First, **BDP-1** would show very strictly confined environment that the intramolecular rotation has been restricted. Second, the intramolecular charge transfer was not the dominant factor to influence the fluorescent emission because in the polar viscous solution, the fluorescent emission was very strong.

### 2.3. Host-guest interaction

With above results in hands, the host-guest supramolecular complex between **BDP-1** and **P[5]** was investigated. $^1$H NMR titration tests were performed to determine the molar ratio of **BDP-1**/**P[5]** complex (Fig. 2). We chose deuterated water and methanol mixture solvents for $^1$H NMR measurement due to bad solubility of **BDP-1** in water. **BDP-1** exhibited well-resolved peaks in both aromatic and aliphatic regions. However, after 0.25 M ratio of **P[5]** addition, the peaks in low field region showed dramatic changes, that is, these peaks became broad, shifted to high field and merged. The terminal methyl group at 5.85 ppm also shifted up-field a little bit. When the molar ratio of **BDP-1**/**P[5]** reached to 1:0.5, these aromatic peaks showed small shift but their intensity decreased further, which indicated the strong host-guest interaction. After molar ratio reached 1:1, no peak shift was observed. This result demonstrated that the supramolecular host-guest complex was formed with 1:1 M ratio. Job plot analysis further confirmed this result (Fig. S3). The binding constant was determined to be 3600 $M^{-1}$.

To further investigate the host-guest complex, 2D NOESY NMR was performed (Fig. 3). Beside the correlation spots between $H_{c,d}$ and $H_{3,\ 6,\ 7}$, two characteristic spots could be clearly observed. The

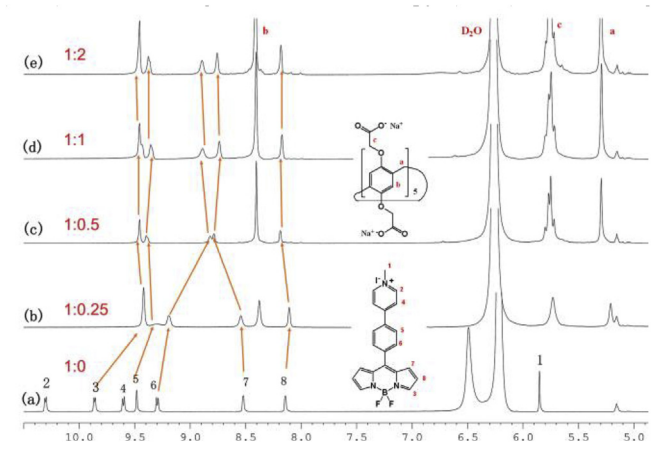


**Fig. 2.** $^1$H NMR titration spectra of complex with varying molar ratio of BDP-1/P[5], (a) 1:0; (b) 1:0.25; (c) 1:0.5; (d) 1:1 and (e) 1:2. Measurement condition: the concentration of BDP-1 is 5 mM, solvent is $D_2O/CD_3OD$ = 4/3.

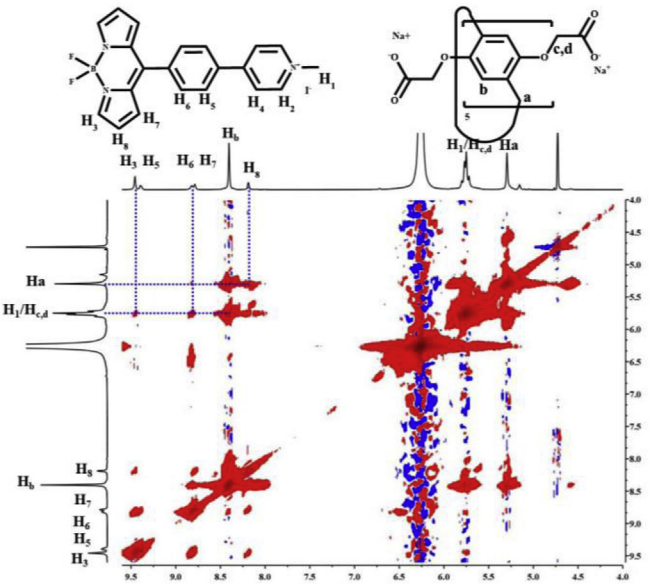


**Fig. 3.** 2D NOESY NMR spectrum of supramolecular complex BDP-1/P[5]. Measurement condition: the concentration of BDP-1 is 5 mM, solvent is $D_2O/CD_3OD$ = 4/3. The molar ratio of BDP-1/P[5] is 1:1.

first one was attributed to correlation from the $H_a$ and $H_8$, which should be strong evidence of the supramolecular complexation because large space existed between the two protons. Another spot was ascribed to $H_b$ and $H_1$, which was merged with $H_c$ and $H_d$. Considering the space between $H_{c,d}$ and $H_b$, this spot should be generated from new supramolecular complex.

### 2.4. Cell imaging

The size and morphology of this supramolecular complex in aqueous solution were investigated by dynamic light scattering (DLS) and scanning electron microscopy (SEM). The average size of the complex aggregate in aqueous is around 190 nm (Fig. 4a), which was further evidenced by the tube morphology from SEM image study (Fig. 4b).

The fluorescence titration measurement was performed by addition **P[5]** to **BDP-1** dilute aqueous solution (Fig. 5). The complex showed gradually enhanced fluorescent intensities with **P[5]** addition. The original emission might from partially aggregate of **BDP-1** due to its bad solubility in water. As **P[5]** addition, the supramolecular host-guest interaction might work and **BDP-1** would be encapsulated to the hydrophobic cavity. Thus, the intramolecular rotation would be restricted, which leads to the enhanced fluorescent emission.

Motivated by the above photophysical studies, cell image tests of

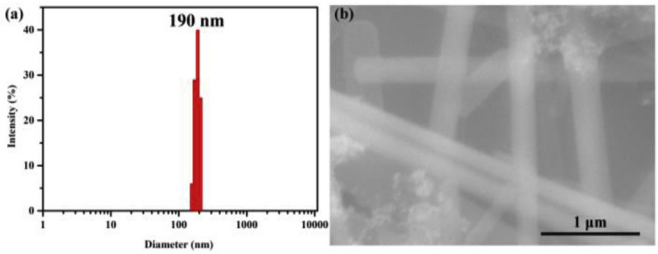


**Fig. 4.** (a) DLS result and (b) SEM image of supramolecular complex BDP-1/P[5] in aqueous solution. Measurement condition: Concentration is 5 mM, molar ratio is 1:1.

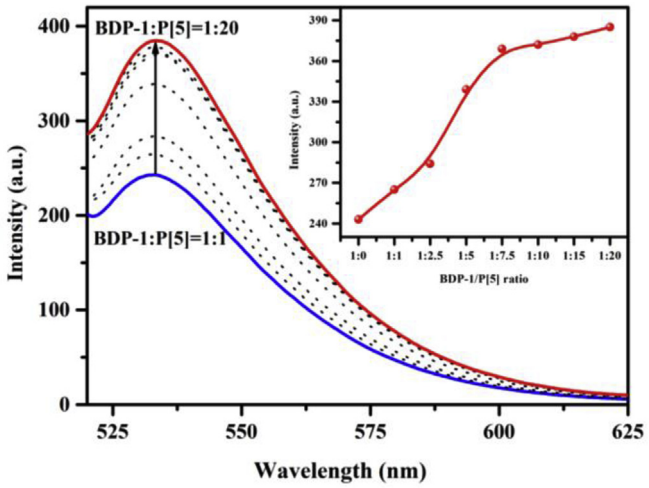


**Fig. 5.** Fluorescent spectra of supramolecular complex BDP-1/P[5] in dilute aqueous solution with increasing molar ratio of P[5]. Condition: BDP-1 concentration is 10 $\mu$M, excitation wavelength is 504 nm, slits are 10 nm/10 nm.

the supramolecular complex were conducted. Michigan Cancer Foundation-7 (MCF-7) cells were selected for bioimaging. After staining these cells for certain time, **BDP-1** and **BDP-1**/**P[5]** complex exhibited apparent intensities difference (Fig. 6). Laser scanning fluorescence microscopy (LSFM) results presented that, after 1 h incubation, **BDP-1** only displayed weak fluorescent spots (Fig. 6b), while the supramolecular complex **BDP-1**/**P[5]** showed strong green emission (Fig. 6e). This result indicated that the strong fluorescent emission came from the supramolecular host-guest interaction. Further detailed observation of the complex cell

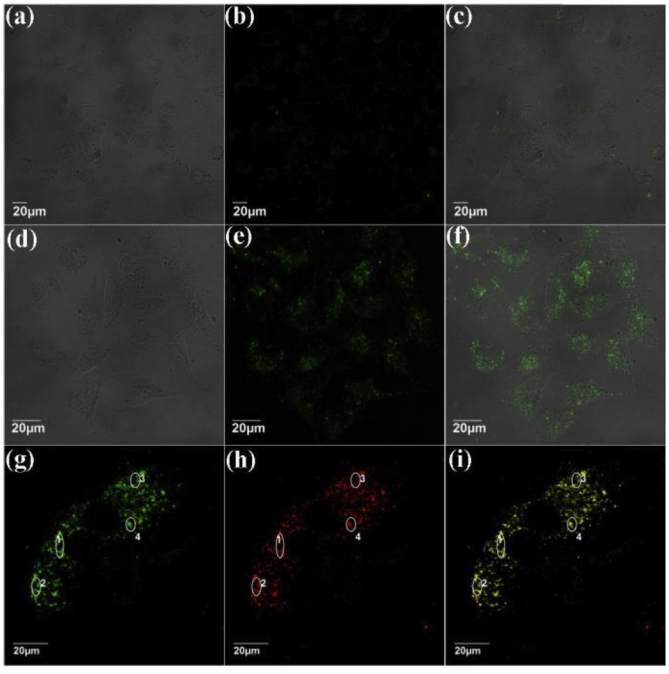


**Fig. 6.** (a, d) Bright-field images, (b, e) confocal luminescence of MCF-7 cells and (c, f) overlay images of the bright-field and the confocal images incubated with BDP-1 and BDP-1/P[5] complex (10 $\mu$M) for 1 h, respectively. Confocal fluorescence images of (g) MCF-7 cells stained with BDP-1/P[5] complex (10 $\mu$M) and (h) Lyso-Tracker Red (LTR, 200 nM). (i) Overlay image of (g) and (h). Excitation wavelength is 515 nm, emission wavelength is from 525 to 545 nm, LTR: Excitation wavelength is 543 nm, emission wavelength is from 580 to 600 nm.

images revealed that the green emissive spots were well dispersed, which implied us that the supramolecular complex might stain specific cell organ. Based on our previous experiences and the positive pyridinium structural moieties, we proposed that these aggregates might stain lysosomes. Therefore, co-staining experiment with the commercial Lyso-Tracker Red (LTR) was performed. The merged yellow image (Region 1, 2, 3 and 4) revealed that our supramolecular complex was lysosome targetable (Fig. 6i), which is consistent with our previous observation for supramolecular polymer [32].

## 3. Conclusions

In summary, a novel BODIPY based supramolecular complex **BDP-1**/**P[5]** was prepared. The host-guest interaction between **BDP-1** and **P[5]** was evidenced by $^1$H NMR titration and 2D NOESY NMR measurements. The fluorescence intensities of the BODIPY dyad were enhanced by increasing solution viscosity or host-guest supramolecular interaction with pillar[5]arenes. Bioimaging studies indicated the supra-molecular complex **BDP-1**/**P[5]** could stain lysosomes specifically. Further studies along this line to prepare other functional BODIPY dyads are undergoing in our laboratory.

## 4. Experimental

### 4.1. Materials

All chemical reagents were commercially available and used as received unless otherwise stated. Dichloromethane (DCM) was dried by standard methods using $CaCl_2$ before distillation. All reactions were performed under nitrogen atmosphere. Analytical thin-layer chromatography (TLC) was performed using TLC plates pre-coated with silica gel (TLC: 10–40 $\mu$m, 0.20 ± 0.03 mm). Flash column chromatography was performed using 40–63 $\mu$m (230–400 mesh) silica gels as the stationary phase. MCF-7 cells were provided by the Institute of Biochemistry and Cell Biology (Chinese Academy of Sciences) and were grown in RPMI 1640 (Roswell Park Memorial Institutes' Medium) at 37 °C under 5% $CO_2$. Commercial Lyso-Tracker Red (LTR) was purchased from Beyotime (China). Confocal fluorescence imaging was performed on an inverted microscope (IX81, Olympus) with a confocal scanning unit (FV1000, Olympus).

### 4.2. Equipments

The $^1$H and $^{13}$C NMR spectra were obtained from a Bruker Advance spectrometer at 500 and 125 MHz, respectively. All chemical shifts were reported in $\delta$ units relative to tetramethylsilane (TMS). A Hitachi U-5100 and Hitachi F-2700 were used to measure UV–vis absorption and fluorescence emission spectra, respectively. High resolution mass spectra were obtained by using a Tsq quantum access max from Thermo. The diameter of the complex was determined at 298 K on ZEN3600 MALVERN via dynamic light scattering (DLS). Scanning electron microscopy (SEM) measurements were conducted in a FEI SIRION200 microscopy with an accelerating voltage of 10 kV.

### 4.3. Synthesis

#### 4.3.1. Synthesis of compound 3

Compound **3** was prepared according to the reported literature. [33] Compound **1** (184 mg, 1 mmol) and solution of $K_2CO_3$ (80 mg, 0.57 mmol, $H_2O$) were added into 1,4-dioxane (60 mL) in flask under $N_2$ atmosphere. The mixture was frozen by liquid nitrogen

and degassed for 5 min. After that, compound **2** (145 mg, 1.2 mmol) was added into flask. After dissolving, the system was frozen, pumped for three times. After this procedures, palladium triphenylphosphine (12 mg, 0.01 mmol) was added into this system. Then the mixture was heated to 110 °C and kept stirring for 20 h. When the system cooled to room temperature, solid was obtained by evaporating the solvents. The crude product was purified by silica gel chromatography with PE: DCM = 1:1 to get brown powder **3** (112 mg, 61%). $^1$H NMR ($CDCl_3$, δ): 7.54 (d, 2H, CH), 7.77 (d, 2H, CH), 8.01 (d, 2H, CH), 8.72 (d, 2H, CH), 10.09 (s, 1H, CH).

*4.3.2. Synthesis of compound 4*

The synthetic procedures were according to our previous works. [34, 35] DCM:PE = 1:3, red powder (31 mg, 16%). $^1$H NMR ($CDCl_3$, δ): 6.56 (d, 2H, CH), 6.96 (d, 2H, CH), 7.56 (d, 2H, CH), 7.68 (t, 2H, CH), 7.78 (t, 2H, CH), 7.85 (s, 2H, CH), 8.72 (d, 2H, CH).

*4.3.3. Synthesis of compound **BDP-1***

Under $N_2$ atmosphere, 4 (31 mg, 0.09 mmol) and iodomethane (1278 mg, 9 mmol) were added into 30 mL acetone in a flask. After that, the system refluxed for 12 h. When the acetone and iodomethane volatilize totally, a tangerine powder **BDP-1** was obtained (43 mg, 98%). $^1$H NMR ($CD_3OD$, δ): 4.45 (s, 3H, CH), 6.67 (d, 2H, CH), 7.04 (d, 2H, CH), 7.90 (d, 2H, CH), 8.02 (t, 2H, CH), 8.21 (s, 2H, CH), 8.51 (s, 2H, CH), 8.98 (d, 2H, CH). 13C NMR ($CD_3OD$, δ): 155.2, 145.2, 144.8, 135.6, 135.1, 134.4, 131.5, 131.1, 128.0, 124.9, 119.6, 59.1. ESI-MS: Calcd. for $C_{21}H_{17}BF_2N_3^+$: 360.1943. Found: 360.2877.

*4.3.4. Synthesis of compound **P[5]***

The synthesis of compound **6** to **9** was according to previous literature.[36] Compound **9** was dissolved in 3 mL water and then the 99 wt% NaOH solution was added into above-mentioned solution dropwise. The dropwise of NaOH stopped when the mixed system changed into clear and colorless. The white solid powder **P[5]** was obtained by vacuum drying (0.25 g, 95%). $^1$H NMR ($D_2O$, δ): 3.92 (s, $CH_2$, 10H), 4.43 (d, $CH_2$, 10H), 4.63 (d, $CH_2$, 10H), 6.85 (s, CH, 10H).[30].

## Declaration of competing interest

The authors declare that they have no known competing financial interests or personal relationships that could have appeared to influence the work reported in this paper.

## Acknowledgements

This work was supported by the State Key Laboratory of Powder Metallurgy, Central South University, the National Natural Science Foundation of China (21501031), the Natural Science Foundation of Hunan (2018JJ2487, 2020JJ4679), the Natural Science Foundation of Jiangxi, China (20151BAB213001), State Key Laboratory of Molecular Engineering of Polymers (Fudan University) and Beijing National Laboratory for Molecular Sciences (BNLMS201829).

## Appendix A. Supplementary data

Supplementary data to this article can be found online at https://doi.org/10.1016/j.tet.2020.131698.

## References

[1] T. Kowada, H. Maeda, K. Kikuchi, Chem. Soc. Rev. 718 (2015) 208–223.
[2] D. Hu, T. Zhang, S. Li, T. Yu, X. Zhang, R. Hu, J. Feng, S. Wang, T. Liang, J. Chen, L.N. Sobenina, B.A. Trofimov, Y. Li, J. Ma, G. Yang, Nat. Commun. 9 (2018) 362.
[3] A. Loudet, K. Burgess, Chem. Rev. 107 (2007) 4891–4893.
[4] A.P. de Silva, T.S. Moody, G.D. Wright, Analyst 134 (2009) 2385–2393.
[5] M. Isik, T. Ozdemir, I.S. Turan, S. Kolemen, E.U. Akkaya, Org. Lett. 15 (2013) 216–219.
[6] T. Matsumoto, Y. Urano, T. Shoda, H. Kojima, T. Nagano, Org. Lett. 9 (2007) 3375–3377.
[7] N. Boens, V. Leen, W. Dehaen, Chem. Soc. Rev. 41 (2012) 1130–1172.
[8] R.R. Hu, E. Lager, A. Aguilar-Aguilar, J. Liu, W.Y. Lam, H.H.Y. Sung, I.D. Williams, Y. Zhong, K.S. Wong, E. Peña-Cabrera, B.Z. Tang, J. Phys. Chem. C 113 (2009) 15845–15853.
[9] M.K. Kuimova, G. Yahioglu, J.A. Levitt, K. Suhling, J. Am. Chem. Soc. 130 (2008) 6672–6673.
[10] M.A.H. Alamiry, A.C. Benniston, G. Copley, K.J. Elliott, A. Harriman, B. Stewart, Y.G. Zhi, Chem. Mater. 20 (2008) 4024–4032.
[11] T.T. Vu, R. Méallet-Renault, G. Clavier, B.A. Trofimov, K. Kiumova, J. Mater. Chem. C 4 (2016) 2828–2833.
[12] L. Wang, Y. Xiao, W. Tian, L. Deng, J. Am. Chem. Soc. 135 (2013) 2903–2906.
[13] R.R. Hu, E. Lager, A. Aguilar-Aguilar, J.Z. Liu, J.W.Y. Lam, H.H.Y. Sung, I.D. Williams, Y.C. Zhong, K.S. Wong, E. Peña-Cabrera, B.Z. Tang, J. Phys. Chem. C 113 (2009) 15845–15853.
[14] R.R. Hu, C.F.A. Gómez-Durán, J.W.Y. Lam, J.L. Belmonte-Vázquez, C. Deng, S. Chen, R.Q. Ye, E. Peña-Cabrera, Y.C. Zhong, K.S. Wong, B.Z. Tang, Chem. Commun. 48 (2012) 10099–10101.
[15] Y. Chen, F. Huang, Z.T. Li, Y. Liu, Sci. China Chem. 61 (2018) 979–992.
[16] J. Gemen, J. Ahrens, L.J.W. Shimon, R. Klajn, J. Am. Chem. Soc. 142 (2020), https://doi.org/10.1021/jacs.0c08589.
[17] Y. Chen, Y. Liu, Chem. Soc. Rev. 39 (2010) 495–505.
[18] S.J. Barrow, S. Kasera, M.J. Rowland, J. del Barrio, O.A. Scherman, Chem. Rev. 115 (2015) 12320–12406.
[19] T. Ogoshi, S. Kanai, S. Fujinami, T.-Aki Yamagishi, Y. Nakamoto, J. Am. Chem. Soc. 130 (2008) 5022–5023.
[20] T. Ogoshi, T.-Aki Yamagishi, Y. Nakamoto, Chem. Rev. 116 (2016) 7937–8002.
[21] C.W. Sathiyajith, R.R. Shaikh, Q. Han, Y. Zhang, K. Meguellati, Y.-W. Yang, Chem. Commun. 53 (2017) 677–696.
[22] L. Shangguan, Q. Chen, B. Shi, F. Huang, Chem. Commun. 53 (2017) 9749–9752.
[23] J. Zhou, B. Hua, L. Shao, H. Feng, G. Yu, Chem. Commun. 52 (2016) 5749–5752.
[24] Y.L. Wu, M. Frasconi, W.G. Liu, R.M. Young, W.A. Goddard III, M.R. Wasielewski, J.F. Stoddart, J. Am. Chem. Soc. 142 (2020) 11835–11846.
[25] H. Wang, Y. Wu, P. Tao, X. Fan, G.-C. Kuang, Chem. Eur J. 20 (2014) 16634–16643.
[26] S. Li, K. Liu, G.-C. Kuang, T. Masuda, A. Zhang, Macromolecules 47 (2014) 3288–3296.
[27] H. Wang, Y. Wu, Y. Shi, P. Tao, X. Fan, X. Su, G.-C. Kuang, Chem. Eur J. 21 (2015) 3219–3223.
[28] l. Yang, Y.-J. Ji, J.-F. Yin, Y. Wu, H. Fan, Y. Zhang, G.-C. Kuang, Soft Matter 12 (2016) 8581–8587.
[29] J.-F. Yin, Y. Hu, D.-G. Wang, Y. Yang, Z. Jin, Y. Zhang, G.-C. Kuang, ACS Macro Lett. 6 (2017) 139–143.
[30] J.-F. Yin, Y. Hu, H. Wang, Z. Jin, Y. Zhang, G.-C. Kuang, Chem. Asian J. 12 (2017) 3088–3095.
[31] X. Ji, J. Chen, X. Chi, F. Huang, ACS Macro Lett. 3 (2014) 110–113.
[32] H. Li, J. Wu, J.-F. Yin, H. Wang, Y. Wu, G.-C. Kuang, Macromol. Rapid Commun. 40 (2019) 1800714.
[33] Chamara A. Gunawardana, Abhijeet S. Sinha, John Desper, Marijana Djakovic, Christer B. Aakeroy, Cryst. Growth Des. 18 (2018) 6936–6945.
[34] D.-G. Wang, F. Song, H. Tang, X.R. Jia, M. Song, G.-C. Kuang, New J. Chem. 41 (2017) 5263–5266.
[35] D.-G. Wang, L.-N. Zhang, Q. Li, Y. Yang, Y. Wu, F. Song, M. Song, G.-C. Kuang, Tetrahedron 73 (2017) 6894–6900.
[36] T. Ogoshi, M. Hashizume, T.-aki Yamagishi, Y. Nakamoto, Chem. Commun. 46 (2010) 3708–3710.